UDC 621.3.014 https://doi.org/10.20998/2074-272X.2025.4.07

D.V. Martynov, Y.V. Rudenko, V.V. Martynov

Improving the operation of an asymmetric inverter with magnetically coupled inductors for energy storage systems

Introduction. Bidirectional DC-DC converters are widely used in energy storage systems for efficient energy transfer. One of the effective converters for such systems is the asymmetric inverter with a magnetically coupled inductors. To enhance the efficiency of this converter for energy storage applications, it is necessary to optimize its parameters. ***Objective****. The objective is to develop a mathematical model of an asymmetric inverter with magnetically coupled inductors and based on this model, to establish the conditions for improving the energy efficiency of the inverter in energy storage systems.* ***Methods****. The study uses the state-space averaging method and simulation modelling to analyse operational processes.* ***Results****. Analytical expressions were derived for calculating current parameters of the magnetically coupled inductor within switching intervals. A correlation was identified between the inductor's inductance and power source parameters under conditions that eliminate circulating currents, thus reducing static energy losses in the inverter.* ***Novelty****. Based on these expressions, new analytical and graphical dependencies were established, illustrating relationships between the inductor parameters and the magnetic coupling coefficient of its windings. These dependencies determine the boundaries of the discontinuous conduction mode for the asymmetric inverter with a magnetically coupled inductors within its switching range.* ***Practical value****. The application of these dependencies during the design phase allows for a reduction in both static and dynamic energy losses in the inverter using discontinuous conduction mode. This will also improve the dynamics of transient processes during changes in the direction of energy flow, which is a significant advantage in the development of hybrid power systems for electric vehicles.* References 19, figures 9.

Key words: **energy storage systems, bidirectional DC-DC converter, asymmetric inverter, magnetic coupling inductors, circulating current.**

Вступ*. В системах накопичення енергії широко використовуються перетворювачі постійної напруги в режимах двонаправленої передачі енергії. Одним з ефективних перетворювальних пристроїв для застосування в таких системах є асиметричний інвертор з магнітозв'язаними індукторами. Для використання вказаного перетворювача в системах енергонакопичення необхідним є удосконалення його параметрів для підвищення ефективності перетворювача.* ***Мета****. Метою є розробка математичної моделі асиметричного інвертора з магнітозв'язаними індукторами та визначення на її основі умов підвищення енергетичної ефективності такого інвертора при застосуванні в системах накопичення енергії.* ***Методи****. При дослідженні процесів в роботі використано метод усереднення в просторі станів та методи імітаційного моделювання.* ***Результати****. Розроблено аналітичні вирази для розрахунків параметрів струмів магнітозв'язаних індукторів на інтервалах комутації, визначено взаємозв'язок між його індуктивністю та параметрами джерел електроживлення, при яких циркуляційні струми відсутні, що зменшує статичні втрати енергії інвертора.* ***Новизна****. На основі розроблених виразів отримано нові аналітичні та графічні залежності між параметрами індуктора та коефіцієнтом магнітного зв'язку між їх обмотками, що визначають межі області переривчастої роботи асиметричного інвертора з магнітозв'язаними індукторами в діапазоні його комутації.* ***Практична значимість****. Використання отриманих залежностей на етапі проектування дозволяє зменшити статичні та динамічні втрати енергії інвертора завдяки використанню режиму переривчастої провідності. Це також дозволить покращити динаміку перехідних процесів при зміни напрямку протікання електроенергії, що є суттєвою перевагою при створенні гібридних систем електроживлення електротранспортних засобів.* Бібл. 19, рис. 9.

Ключові слова: **системи накопичення електроенергії, двонаправлений перетворювач постійної напруги, асиметричний інвертор, магнітозв'язані індуктори, циркулюючий струм.**

Introduction. Batteries and supercapacitors are the most common and economical choices for energy storage today. This drives strong demand for bidirectional DC-DC converters, which facilitate energy transfer between storage units and power-consuming devices. These converters support bidirectional energy flow and flexible control across all modes of operation, making them integral to a range of energy systems, such as hybrid and fuel cell vehicles, renewable energy system, and beyond [1–3]. In renewable energy systems, a bidirectional DC-DC converter is used to combine different types of energy sources [4–14], with different voltage levels, providing a quick response when changing the direction of the electricity flow.

Currently, numerous circuit topologies for the potential implementation of bidirectional DC-DC converters are known [5–18]. These topologies are primarily classified into two types: non-isolated and isolated converters, each suited to specific applications.

A typical structure of a non-isolated bidirectional DC-DC converter combines a buck converter and a boost converter in a half-bridge configuration [4, 9, 13]. These converters can operate independently to create a bidirectional flow of electrical energy, although this leads to inefficient use of electromagnetic components and power switches. However, unidirectional DC-DC converters can be configured as bidirectional converters based on the half-bridge inverter topology by utilizing the built-in diodes within the switches and shared inductance. There are several disadvantages to the half-bridge inverter topology when used as a bidirectional converter. Firstly – excessive energy losses. Significant energy losses occur due to diode reverse recovery or faulty simultaneous conduction of both switches, which can lead to device failure. The conventional solution is to introduce dead time into the switching interval. However, this approach leads to duty cycle losses and limits the switching frequency. Secondly – poor transient response. The shared inductance used for current ripple smoothing negatively affects the dynamic response during changes in the direction of power flow, which is a major issue for hybrid power systems. This problem arises due to a reduction in stored energy, for example during the transition to regenerative breaking in electric vehicle power systems [4].

Many studies have been done to research bidirectional converters with efficient power flow management [7–15], as well as various control strategies to improve power quality. Recently, new converters based on an asymmetric inverter with magnetically coupled inductors have been introduced as an alternative to traditional bidirectional DC-DC converter topologies [4, 9, 15]. These structures have been applied in various applications due to their immunity to short-circuit issues and low losses during diode reverse recovery. This unique characteristic is achieved using magnetically coupled inductors and the structure of the asymmetric inverter, such as the dual buck inverter and the split-phase PWM inverter. The converter offers two key advantages: firstly, shoot-through currents are avoided because no active power switches are connected in series in each phase's arm; secondly, energy dissipation during the reverse recovery of the power switch is significantly reduced, as discrete diodes with superior dynamic characteristics compared to the internal diodes of power switches can be utilized.

The bidirectional converter using the topology of an asymmetric inverter with magnetically coupled inductors is shown in Fig. 1.

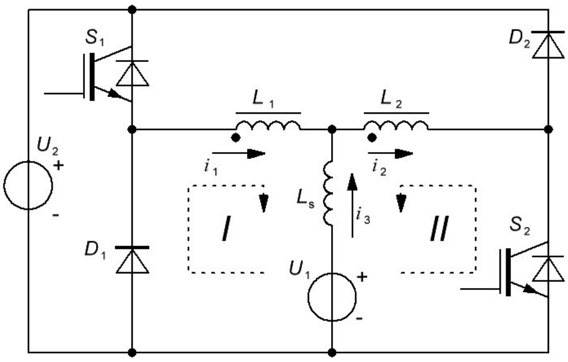

Fig. 1. Schematic of the bidirectional converter based on the topology of an asymmetric inverter with magnetically coupled inductors

The device consists of four switches, of which switches S_1 and S_2 are controllable. This converter topology allows operation in both buck and boost modes in both directions of power flow. When transferring energy from source U_2 to U_1, switch S_1 is activated while S_2 remains OFF; conversely, during energy transfer in the reverse direction from source U_1 to U_2, switch S_2 is activated.

The converter has some disadvantages when using a magnetically coupled inductor, especially when there is a significant voltage difference between the low-voltage and high-voltage sides. In this scenario, circulating currents may arise during certain operating modes of the converter [4], resulting in power loss.

Research has shown that the presence of circulating currents increases the static energy losses in the inverter. On the other hand, the efficiency of the inverter also depends on the dynamic energy losses. Dynamic power dissipation is reduced by operating in discontinuous conduction mode, which allows transistors to switch at zero current.

To date, research aimed at reducing circulating currents, improving transient response quality and increasing energy efficiency has mainly focused on modifying the structure of the asymmetric inverter or implementing new control methods [12, 13, 15, 17]. While structural modifications or the implementation of advanced control strategies can partially solve these issues, they also have certain disadvantages, such as an increased number of components, greater circuit complexity and higher energy losses. In addition, the implementation of new control methods increases the complexity of the control system. Analysis of the processes in inverters shows that the use of non-magnetically coupled inductors prevents the occurrence of circulating currents but also eliminates one of the main advantages of the asymmetric inverter, which is the fast transition dynamics between energy storage and discharge modes [15, 16]. Also, the use of counter-rotating inductor windings does not provide significant benefits due to the complexity of additional filtering systems [17]. It is known that in an asymmetric inverter with non-magnetically coupled inductors, circulating currents are absent; however, this leads to slow transient processes when changing the direction of power flow. Inverter structures with magnetically coupled inductors provide good speed during changes in power flow direction; nevertheless, under certain parameter ratios of the power sources on the low-voltage and high-voltage sides [4], circulating currents may arise [17]. Thus, it can be concluded that a strong magnetic coupling in the inductor leads to circulating currents, while the absence of magnetic coupling prevents them. These studies do not consider the relationship between an asymmetrical inverter's parameters, its magnetically coupled inductors, and the parameters of additional inductive filters (additional inductor) that can minimise circulating current.

In this work, we focus on the elimination of some disadvantages of the asymmetric inverter with magnetically coupled inductors and additional inductor (Fig. 1) by developing analytical expressions for the calculation and rational selection of effective parameters when used in a bidirectional DC-DC converter for energy storage systems. Solving these problems is expected to improve the overall energy efficiency of the asymmetric inverter. Furthermore, the use of analytical expressions will simplify the design and development of the asymmetric inverter for energy storage applications.

The **objective** of this work is to develop a mathematical model of an asymmetric inverter with magnetically coupled inductors, and based on this model, to determine the conditions for increasing the energy efficiency of such an inverter when used in energy storage systems.

Methods. To solve this problem, we need to optimise the parameters of magnetic coupling inductors, at which sufficient performance is kept, and the current circulation tends to zero. We will also find the ratio of the converter parameters at which it can operate in the intermittent conduction mode.

The study of the asymmetric inverter with magnetically coupled inductors was performed by analysing its operating modes using the PSIM circuit simulation software, based on the developed simulation model shown in Fig. 1. This model included magnetically coupled inductors with $L_1 = L_2 = 30$ μH and an additional inductor of $L_s = 6$ μH, designed to block unwanted circulating current. It was assumed that the switching elements of the converter operate instantaneously, the active resistance in the open state is zero, and the active resistance of the inductor winding is also zero. In the circuit illustrated in Fig. 1, the supply voltage $U_2 > 2U_1$.

In Fig. 2, the calculated results of the currents are presented: $i_1(t)$ is the current through inductor L_1, $i_2(t)$ is the current through inductor L_2, and $i_3(t)$ is the current through inductor L_s in the circuit shown in Fig. 1, during the operation of the bidirectional converter in the mode of discontinuous currents.

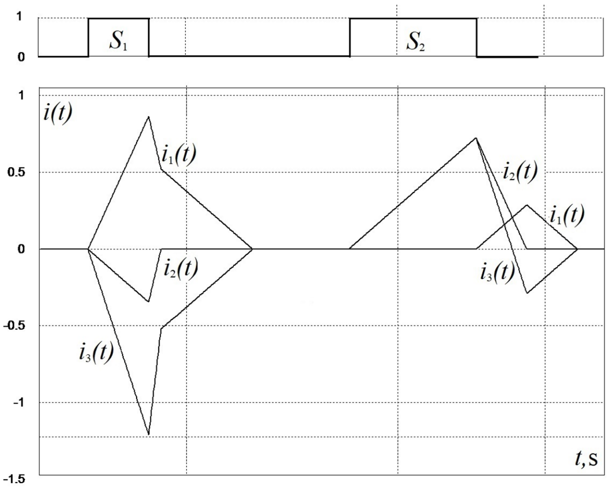

Fig. 2. Graph of the calculated current results during the operation of the bidirectional converter in the discontinuous mode

When transferring energy from source U_2 to U_1, the circuit operates as a buck regulator with the active transistor S_1. During the energy accumulation phase, with transistor S_1 in the ON state, voltage U_2 is applied to the inductors L_1=L_2. Due to the magnetic coupling of the inductors, the voltage at L_2 at the connection point of inductor L_s exceeds U_1, resulting in circulating current through the diode of transistor S_2 and inductor L_2. This increases static losses due to the current flowing through the antiparallel diode of transistor S_2. When the transistor is turned OFF, circulating current is absent, as shown in Fig. 2. This indicates that blocking the antiparallel diode in transistor S_2 prevents circulating current; however, it causes additional static losses in the converter. The path of the circulating current in the active mode of transistor S_1 is represented in Fig. 1 by the dashed contour *II*.

When transferring energy from source U_1 to source U_2, the circuit operates as a boost regulator with transistor S_2. During the activation of transistor S_2, voltage U_1 is applied to inductor L_2, and when the voltage U_1 is less than U_2, circulating current is absent. When transistor S_2 is turned OFF, as shown in Fig. 3, circulating current flows through diode D_1 and the inductor L_1, as the voltage $U_2/2>U_1$ is induced on the inductor L_1.

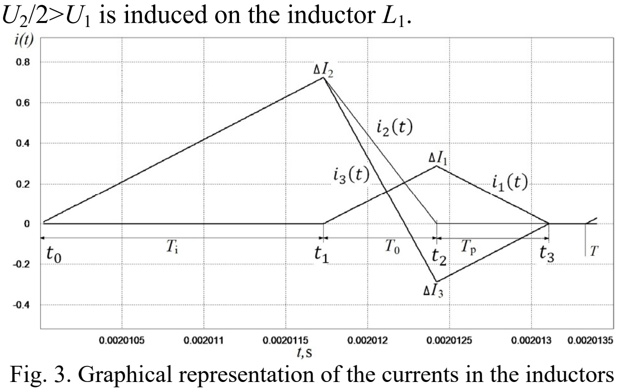

Fig. 3. Graphical representation of the currents in the inductors of the asymmetric inverter during the energy transfer period from the low-voltage source to the high-voltage source in the discontinuous mode

The appearance of the circulating current $i_1(t)$ in Fig. 2 leads to the fact that a part of the energy from the source U_1, accumulated in the inductor L_2 when the transistor S_2 is open, does not enter the source U_2. The path of the circulating current after transistor S2 is turned OFF is shown in Fig. 1 by the dashed contour *I*.

Let's analyze what occurs in the inverter when transistor S_2 operates in active mode. As shown by the calculations in Fig. 3, when the inverter is operating, for example in boost mode with discontinuous inductor currents, four continuous operating intervals of the circuit shown in Fig. 1 can be identified: the first interval, $T_i(t_0–t_1)$, occurs when the transistor S_2 is open while all other switches are OFF; the second interval $T_0(t_1–t_2)$ during the pause in the operation of transistor S_2; the third interval $T_p(t_2–t_3)$ during the time of reduction of inductor currents to zero; the fourth interval $(t_3–T)$ is the cutoff when all the switches of the converter are closed.

The presence of three intervals during pauses in transistor control is influenced by the coupling of the inductors and the voltage ratios of the power sources. An analysis of the time diagrams in Fig. 3 shows that the waveforms of the converter state variables – currents i_1, i_2, i_3 – exhibit a multistep character with several sequential stages of rise and fall, while the current i_2 demonstrates a varying sign.

The configurations of the equivalent circuits during the intervals of interest T_i, T_0 and T_p (Fig. 3), are shown in Fig. 4 – 6. Figure 4 shows the interval T_i, where the transistor S_2 is turned ON. Figure 5 shows the interval T_0, after the transistor S_2 has been switched OFF, during which the current $i_3(t)$ decreases to zero. Figure 6 shows the interval T_p the scenario in which the energy stored in the inductor by the circulating current is returned to the power source U_1.

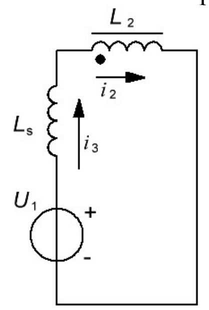

Fig. 4. Equivalent circuit during the time interval T_i

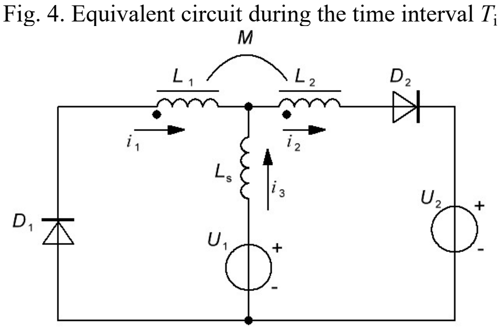

Fig. 5. Equivalent circuit during the time interval T_0

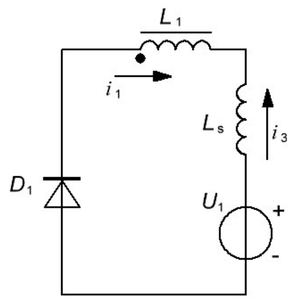

Fig. 6. Equivalent circuit during the time interval T_p

We will define the parameters of the equivalent circuits for which the circulating currents are negligible. To analyse the processes, we will use the converter model obtained by the averaging method developed in [19]. Accordingly, we will establish a system of differential equations for the three switching intervals:

$$\begin{cases} L_2 \dfrac{\mathrm{d}i_2}{\mathrm{d}t} + L_s \dfrac{\mathrm{d}i_2}{\mathrm{d}t} = U_1; \\ -L_2 \dfrac{\mathrm{d}i_1}{\mathrm{d}t} + M \dfrac{\mathrm{d}i_2}{\mathrm{d}t} - L_s \dfrac{\mathrm{d}i_3}{\mathrm{d}t} = U_1; \\ U_1 + L_s \dfrac{\mathrm{d}i_3}{\mathrm{d}t} + L_2 \dfrac{\mathrm{d}i_2}{\mathrm{d}t} - M \dfrac{\mathrm{d}i_1}{\mathrm{d}t} = U_2; \\ L_1 \dfrac{\mathrm{d}i_1}{\mathrm{d}t} + L_s \dfrac{\mathrm{d}i_1}{\mathrm{d}t} = U_1. \end{cases} \quad (1)$$

We will move to a system of algebraic equations with averaged variables concerning the currents i_1, i_2 and i_3, taking into account the signs of the increments of the state variable functions during the switching intervals of the converter. Using the state-space averaging method based on Lagrange's theorems [19], we can express the system of algebraic equations as follows:

$$\begin{cases} L_2 \dfrac{\Delta I_2}{T_i} + L_s \dfrac{\Delta I_2}{T_i} = U_1; \\ -L_1 \dfrac{\Delta I_1}{T_0} + M \dfrac{\Delta I_2}{T_0} - L_s \dfrac{\Delta I_3}{T_0} = U_1; \\ U_1 + L_s \dfrac{\Delta I_3}{T_0} + L_2 \dfrac{\Delta I_2}{T_0} - M \dfrac{\Delta I_1}{T_0} = U_2; \\ L_1 \dfrac{\Delta I_1}{T_p} + L_s \dfrac{\Delta I_1}{T_p} = U_1; \\ \Delta I_1 + \Delta I_2 = \Delta I_3, \end{cases} \quad (2)$$

where ΔI_1, ΔI_2, ΔI_3 are the increments of the corresponding state variable functions during the converter's switching intervals, equal to the ripple of these functions; $M=K_{\text{cop}}\sqrt{L_1 \cdot L_2}$ is the mutual inductance between the inductors; K_{cop} is the magnetic coupling coefficient between the inductors; T_{i} is the specified duration of the first interval; T_0 is the duration of the second interval; T_{p} is the duration of the third switching interval.

For further analysis of the processes in the converter, it is necessary to solve the obtained system of algebraic equations (2) with respect to the independent variables. The solution to this system is given by the following equations:

$$\Delta I_1 = T_i \frac{U_1}{(L_2 + L_s)} \cdot \frac{(M + L_2)U_1 + (L_s - M)U_2}{(M + L_1)U_1 - (L_s + L_1)U_2}; \quad (3)$$

$$\Delta I_2 = T_i \frac{U_1}{L_2 + L_s}; \quad (4)$$

$$\Delta I_3 = T_i \frac{U_1}{(L_2 + L_s)} \cdot \frac{(2M + L_1 + L_2)U_1 - (L_1 - M)U_2}{(M + L_1)U_1 - (L_s + L_1)U_2}; \quad (5)$$

$$T_0 = T_i \frac{U_1}{(L_2 + L_s)} \cdot \frac{\left(L_2 L_1 + L_s L_2 + L_1 L_s + 2ML_s - M^2\right)}{(L_s + L_1)U_2 - (M + L_1)U_1}; \quad (6)$$

$$T_p = T_i \frac{(L_1 + L_s)}{(L_2 + L_s)} \cdot \frac{(M + L_2)U_1 + (L_s - M)U_2}{(M + L_1)U_1 - (L_s + L_1)U_2}. \quad (7)$$

Considering the case close to ideal magnetic coupling between the inductors $M \sim L_1 = L_2 = L$, we will find the relationship of parameters under which the current increase ΔI_1 in Fig. 3 approaches zero during the second interval. We express (3) in a simplified form as:

$$\Delta I_1 = T_i \frac{U_1}{(L + L_s)} \cdot \frac{2LU_1 + (L_s - L)U_2}{2LU_1 - (L_s + L)U_2}. \quad (8)$$

Setting (8) equal to zero, we can determine the value of the additional inductor L_{s} at which the increase in circulating current approaches zero.

$$L_s = L \frac{U_2 - 2U_1}{U_2}. \quad (9)$$

Using the notation $k=U_2/U_1$, we transform (9) to the following form:

$$\frac{L_s}{L} = 1 - \frac{2}{k}. \quad (10)$$

According to (10), as the difference between the power sources $U_2 >> U_1$ increases, a larger additional inductance is required to prevent current circulation in the asymmetric inverter. Figure 7 shows the graphical solution of (10).

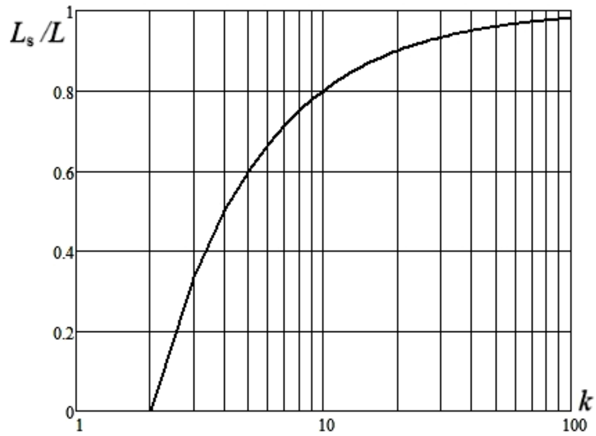

Fig. 7. Graphical interpretation of the dependence of additional inductance on the voltage ratio of power sources

From the analysis of the graph in Fig. 7, it follows that if the voltage of source U_2 is twice as large as the voltage of source U_1, then the additional inductor L_{s}, to reduce the current circulation in the asymmetric inverter, can be omitted. If the voltage source U_2 significantly exceeds the voltage source U_1, the value of the additional inductor tends to the value of the magnetically coupled inductors $L_{\text{s}}=L_1=L_2=L$.

To achieve high power density, bidirectional DC-DC converters often use the discontinuous mode, which allows the inductor to be minimised in size. The current ripple associated with this mode can be minimised either by employing multiphase configurations in power supply systems or by utilizing large energy storage devices. In particular, in hybrid electric vehicle power systems, energy storage is implemented using various batteries, supercapacitors, and generally large capacitive storage solutions. Another significant advantage of operating in discontinuous conduction mode is the zero losses during turn-on, resulting in low losses during the diode's reverse recovery.

The condition for the existence of discontinuous conduction mode in the converter is that the sum of the durations of its switching intervals must be less than the duration of the switching period. The limiting condition is when the sum of the durations of the intervals equals the duration of the switching period T, which leads to the following equation:

$$T_i + T_0 + T_p = T \, . \tag{11}$$

Using the parameter values from (3–7), we obtain the sum of the durations of the switching intervals:

$$T_i + T_0 + T_p = \frac{L_2 + M}{L_2 + L_s} T_i \, , \tag{12}$$

and the condition for the existence of the discontinuous conduction mode of the converter:

$$\frac{L_2 + M}{L_2 + L_s} T_i < T \, . \tag{13}$$

Let's consider the following relationship $\gamma = T_i/T$, $M = L_1 \cdot (K_{cop}/K_{tr})$, $L_2 = L_1/K_{tr}^2$, γ is the duty cycle of the converter's control pulses; K_{tr} is the transformation ratio between the coupled inductors. In this case, we can express the condition for the existence of discontinuous conduction mode as follows:

$$\frac{L_1 \left(1 + K_{tr} K_{cop}\right)}{L_1 + K_{tr}^2 L_s} \gamma < 1 \, . \tag{14}$$

Let's express the relationship between the inductors L_1 and L_2 using the parameter $\alpha = L_1/L_s$. From (14), we can derive the following formula in relative units concerning this parameter:

$$\alpha < \frac{K_{tr}^2}{\left(1 + K_{tr} K_{cop}\right)\gamma - 1} \, . \tag{15}$$

Equation (15) defines the relationships between the inductance values L_1 and L_s across the entire range of the converter's switching operation that ensures the operation in discontinuous conduction mode.

In the graphical representation, the condition derived in (15) corresponds to the range of values left and below the thresholds shown in Fig. 8.

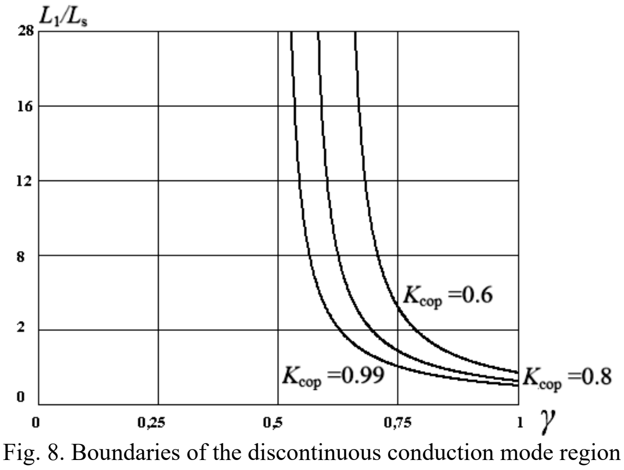

Fig. 8. Boundaries of the discontinuous conduction mode region as a function of the duty cycle of the control pulses of the converter for different values of the magnetic coupling coefficient between the inductors

In Fig. 8, the boundary values are depicted for K_{tr}=1, as well as for several values of the magnetic coupling coefficient between the inductors. From the analysis of (14) and the graphs in Fig. 8, in the switching modes when γ<0.5, the converter maintains the discontinuous conduction mode regardless of the magnetic coupling coefficient and the relationship between the inductors L_1 and L_s. Where L_1=L, L has been described above for use in the expression (8–10).

Figure 9 shows the simulation results of a bidirectional converter based on the asymmetric inverter circuit with the following parameters: L_1=L_2=15 µH, PWM modulation frequency is 300 kHz, power supplies U_1=14 V, U_2=56 V. According to (7), the additional inductance value is L_s=8.57 µH.

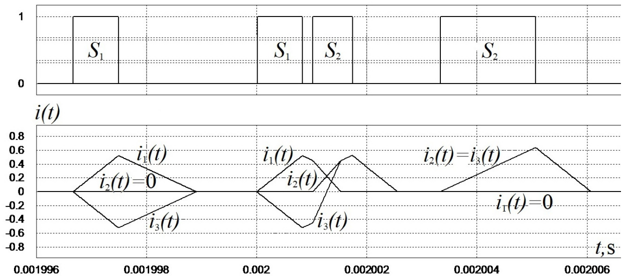

Fig. 9. The results of current calculations during the operation of a bidirectional converter with an additional inductor, whose parameters are determined by (7)

As can be seen from the simulation results, there are no circulating currents. Despite the presence of the additional inductor, the high-speed performance is maintained when the direction of energy transfer is changed. The work has therefore allowed the relationship to be established between the key parameters of the asymmetric converter with additional inductor to prevent circulating currents in an ideal magnetically coupled inductors.

Conclusions.

1. The new analytical model of an asymmetric inverter with magnetically coupled inductors for energy storage systems has been developed, along with a methodology for calculating its parameters. The derived analytical expressions allow the inverter parameters to be calculated at the design stage, ensuring improved efficiency.
2. The method for improving the structure of the asymmetric inverter with magnetically coupled inductors has been proposed, using an additional inductor to reduce undesirable circulating currents in the converter, that lead to power losses. The schematic implementation of the inductor connection has been determined, as well as the relationship between their inductance and the ratio of the power supply voltages, under which circulating currents are absent in the asymmetric inverter, reducing the static energy losses in the device. It was found that the higher the voltage of the high voltage power supply exceeds the low voltage power supply, the greater the additional inductance that needs to be added to prevent circulating currents in the asymmetric inverter with magnetically coupled inductors.
3. Analytical expressions and calculation methods for the converter parameters have been developed to ensure its ability to operate in discontinuous conduction modes. Such modes contribute to the reduction of dynamic losses in the converter, leading to an increase in the performance of the asymmetric converter by reducing switching losses.

It has been found that the asymmetric converter maintains the discontinuous conduction mode regardless of the magnetic coupling coefficient and the ratio between the inductance of the inductors and the additional inductance, provided that the relative duration of the control pulses is less than 0.5.

The simulation carried out confirms the reliability of the results obtained.

Acknowledgment. The work was carried out by the budget program on the topic «Source-4» state registration number 0124U000393 (KPKVK 6541030).

Conflict of interest. The authors declare that they have no conflicts of interest

REFERENCES

1. Zharkin A., Novsky V., Martynov V., Pazieiev A. Provision of high quality power supply in distribution networks with renewable energy sources. *Bulletin of NTU "KhPI". Series: Electric machines and electromechanical energy conversion*, 2019, no. 20 (1345), pp. 4-13. (Ukr). doi: https://doi.org/10.20998/2409-9295.2019.20.01.

2. Hein K., Xu Y., Wilson G., Gupta A. K. Coordinated Optimal Voyage Planning and Energy Management of All-Electric Ship With Hybrid Energy Storage System. *IEEE Transactions on Power Systems*, 2021, vol. 36, no. 3, pp. 2355-2365. doi: https://doi.org/10.1109/TPWRS.2020.3029331.

3. Fonseca de Freitas C. A., Bartholomeus P., Margueron X., Le Moigne P. Partial Power Converter for Electric Vehicle Hybrid Energy Storage System Using a Controlled Current Source Cascade Architecture. *IEEE Access*, 2024 vol. 12, pp. 150898-150913. doi: https://doi.org/10.1109/ACCESS.2024.3477935.

4. Yurchenko O.M., Martynov D.V., Martynov V.V. Research of a bidirectional voltage converter for application in energy storage system. *Proceedings of the Institute of Electrodynamics of the National Academy of Sciences of Ukraine*, 2023, no. 65, pp. 121-126. (Ukr). doi: https://doi.org/10.15407/publishing2023.65.121.

5. El Fadil H., Giri F. Sliding Mode Control of Fuel Cell and Supercapacitor Hybrid Energy Storage System. *IFAC Proceedings Volumes*, 2012, vol. 45, no. 21, pp. 669-674. doi: https://doi.org/10.3182/20120902-4-FR-2032.00117.

6. Cosso S., Benevieri A., Marchesoni M., Passalacqua M., Vaccaro L., Pozzobon P. A New Topology of Multi-Input Bidirectional DC-DC Converters for Hybrid Energy Storage Systems. *Energies*, 2024, vol. 17, no. 20, art. no. 5120. doi: https://doi.org/10.3390/en17205120.

7. Hosseinzadeh M.A., Sarebanzadeh M., Garcia C.F., Babaei E., Rodriguez J. An Asymmetric Switched-Capacitor Multicell Inverter With Low Number of DC Source and Voltage Stress for Renewable Energy Source. *IEEE Access*, 2022, vol. 10, pp. 30513-30525. doi: https://doi.org/10.1109/ACCESS.2022.3140786.

8. Passos Nascimento A.J., Ferro de Menezes B., Jo de Mesquita S., Rabelo Costa K., Lessa Tofoli F., Daher S., Marcelo Antunes F.L. Bidirectional Isolated Asymmetrical Multilevel Inverter. *IEEE Transactions on Circuits and Systems II: Express Briefs*, 2023, vol. 70, no. 1, pp. 151-155. doi: https://doi.org/10.1109/TCSII.2022.3201601.

9. Meng Z., Wang Y.-F., Yang L., Li W. High Frequency Dual-Buck Full-Bridge Inverter Utilizing a Dual-Core MCU and Parallel Algorithm for Renewable Energy Applications. *Energies*, 2017, vol. 10, no. 3, art. no. 402. doi: https://doi.org/10.3390/en10030402.

10. Akbar F., Khan U.A., Khan A.A., Ahmed H.F., Elkhateb A., Cha H., Park J.-W. Dual-Buck Three-Switch Leg Converters With Reduced Number of Passive Components. *IEEE Transactions on Power Electronics*, 2022, vol. 37, no. 11, pp. 13484-13498. doi: https://doi.org/10.1109/TPEL.2022.3183834.

11. Lyu D., Sun Y., Teixeira C.A., Ji Z., Zhao J., Wang Q. A Modular Multilevel Dual Buck Inverter With Adjustable Discontinuous Modulation, *IEEE Access*, 2020, vol. 8, pp. 31693-31709. doi: https://doi.org/10.1109/ACCESS.2020.2972906.

12. Bui D-V., Cha H. Nguyen V-C. Asymmetrical PWM Scheme Balancing Voltages Dual-outputs Interleaved Four-switch Buck-Boost DC-DC Converter. *2022 IEEE Ninth International Conference on Communications and Electronics (ICCE)*, 2022, pp. 482-487. doi: https://doi.org/10.1109/ICCE55644.2022.9852055.

13. Mirza A.B., Emon A.I., Vala S.S., Luo F.A Comprehensive Analysis of Current Spikes in a Split-Phase Inverter. *2022 IEEE Applied Power Electronics Conference and Exposition (APEC)*, 2022, pp. 1580-1585. doi: https://doi.org/10.1109/APEC43599.2022.9773407.

14. Yao Z. Review of Dual-Buck-Type Single-Phase Grid-Connected Inverters. *IEEE Journal of Emerging and Selected Topics in Power Electronics*, 2021, vol. 9, no. 4, pp. 4533-4545. doi: https://doi.org/10.1109/JESTPE.2020.3027770.

15. Patarroyo-Gutierrez L.D., Hernández Gómez O.M., Jiménez López F.R. El inversor dual buck de inductor simple: control de voltaje y procedimiento para obtener su modelo matemático. *Revista EIA*, 2024, vol. 21, no. 41, art. no. 4117, pp. 1-21. (Esp). doi. https://doi.org/10.24050/reia.v21i41.1692.

16. Bui V.-D., Cha H. Asymmetrical PWM split-phase boost PWM AC-AC converter with inherent output voltage balancing. *Journal of Power Electronics*, 2024, vol. 24, no. 1, pp. 20-31. doi: https://doi.org/10.1007/s43236-023-00717-w.

17. Guo S., Huang A.Q. Control and analysis of the high efficiency split phase PWM inverter. *2014 IEEE Applied Power Electronics Conference and Exposition - APEC 2014*, 2014, pp. 2415-2420. doi: https://doi.org/10.1109/APEC.2014.6803641.

18. Kumar R.S., Reddy C.S.R., Chandra B.M. Optimal performance assessment of intelligent controllers used in solar-powered electric vehicle. *Electrical Engineering & Electromechanics*, 2023, no. 2, pp. 20-26. doi: https://doi.org/10.20998/2074-272X.2023.2.04.

19. Rudenko Y. Analysis of DC-DC Converters by Averaging Method based on Lagrange Theorems. *2021 IEEE 2nd KhPI Week on Advanced Technology (KhPIWeek)*, 2021, pp. 367-370. doi: https://doi.org/10.1109/KhPIWeek53812.2021.9570089.

Received 30.10.2024
Accepted 20.02.2025
Published 02.07.2025

D.V. Martynov[1], *PhD Student,*
Y.V. Rudenko[1], *Doctor of Technical Science,*
V.V. Martynov[1], *Doctor of Technical Science,*
[1] Institute of Electrodynamics of the National Academy of Sciences of Ukraine,
56, Prospect Beresteiskyi, Kyiv, 03057, Ukraine,
e-mail: d.martynov@electrotechimpulse.com (Corresponding Author); mart_v@ied.org.ua; rudenko@ied.org.ua

How to cite this article:
Martynov D.V., Rudenko Y.V., Martynov V.V. Improving the operation of an asymmetric inverter with magnetically coupled inductors for energy storage systems. *Electrical Engineering & Electromechanics*, 2025, no. 4, pp. 53-58. doi: https://doi.org/10.20998/2074-272X.2025.4.07